Korea-Australia Rheology Journal
Vol. 11, No. 3, September 1999 pp.233-240

Dynamic simulation of squeezing flow of ER fluids using parallel processing

Do Hoon Kim, Sang-Hyon Chu, Kyung Hyun Ahn* and Seung Jong Lee**
School of Chemical Engineering and Institute of Chemical Processes
Seoul National University, Seoul 151-742, Korea
**R&D Center, Cheil Industries Inc., Euiwang-shi*
Kyunggi-do 437-010, Korea

(Received May 19, 1999; final revision received July 29, 1999)

Abstract

In order to understand the flow behavior of Electrorheological (ER) fluid, dynamic simulation has been intensively performed for the last decade. When the shear flow is applied, it is easy to carry out the simulation with relatively small number of particles because of the periodic boundary condition. For the squeezing flow, however, it is not easy to apply the periodic boundary condition, and the number of particles needs to be increased to simulate the ER system more realistically. For this reason, the simulation of ER fluid under squeezing flow has been mostly performed with some representative chains or with the approximation that severely restricts the flow geometry to reduce the computational load. In this study, Message Passing Interface (MPI), which is one of the most widely-used parallel processing techniques, has been employed in a dynamic simulation of ER fluid under squeezing flow. As the number of particles used in the simulation could be increased significantly, full domain between the electrodes has been covered. The numerical treatment or the approximation used to reduce the computational load has been evaluated for its validity, and was found to be quite effective. As the number of particles is increased, the fluctuation of the normal stress becomes diminished and the prediction in general was found to be qualitatively in good agreement with the experimental results.

Key words : Electrorheological fluid, Squeezing flow, Parallel processing, Normal stress, Yield stress

1. Introduction

Electrorheological (ER) fluid shows dramatic change in rheological properties when an electric field is applied. The response is so fast that the change of viscosity usually occurs in several milliseconds. ER fluid, the dispersion of polarizable particles in an insulating base medium, shows orders-of-magnitude change in apparent viscosity with the application of just a few watts of electric power. Most of research has been made to enhance the ER properties by searching for a new material. However in addition to these efforts, it is also necessary to pay attention to a better design of ER devices to ensure the desired properties.

As far as the performance of ER fluid is concerned, the flow condition is very important. Couette flow, Poiseuille flow, and squeezing flow are typical flows in general. ER fluid shows yield stresses in the order of Couette < Poiseuille < squeezing flow [Havelka and Pialet (1996)]. Stresses in squeezing flow can be orders of magnitude higher than those in pure shear flow [Brooks (1994), Sproston *et al.* (1991)]. Therefore, the use of ER fluids under squeezing flow has attracted much attention recently.

In a previous paper [Kim *et al.* (1999)], a dynamic simulation technique was employed to investigate the dynamic response of ER fluids under squeezing flow. Unlike the simulation under shear flow where it is easy to carry out the simulation with relatively small number of particles due to the periodic boundary condition, the simulation under squeezing flow is not easy to apply the periodic boundary condition and the number of particles needs to be increased to simulate the ER system more realistically. For this reason, the simulation of ER fluid under squeezing flow has been mostly performed with some representative chains or with the approximation that severely restricts the flow geometry to reduce the computational load. In the case of isolated chain models, in which a single and multiple chains are formed and investigated as a part of the whole domain between the electrodes, small peaks in normal stress curve could be observed, which result from the transition of the configuration from an unstable to a stable state and vice versa. According to this result, single chain

**Corresponding author: sjlee@plaza.snu.ac.kr

seems to be more effective than the multiple chain in terms of the normal stresses. This result agreed with that of Lukkarinen and Kaski (1998). The approximation of "Piece-of-cake" (POC) was also introduced to lessen the computational load. This approximation which accounts only for the part of the whole domain between the electrodes simulates the ER behavior reasonably well at a much reduced computational load. It shows a yield behavior (in the zz-component of the stress tensor), the overshoot at an initial state, and the development of normal stress, however, it needs to be carefully evaluated because of its artificial treatment of the boundary condition.

In this paper, Message Passing Interface (MPI), which is one of the most widely-used parallel processing techniques, has been employed in a dynamic simulation of ER fluid under squeezing flow in order to consider the whole domain between the electrodes with a large number of particles. The POC approximation has been intensively evaluated, and the macroscopic as well as microscopic behavior of ER fluid under squeezing flow has been investigated in the whole space between the electrode disks. Finally the numerical prediction of ER behavior was compared with the previous experimental results.

2. Theory

The ER fluid to be treated in this study is a simple system composed of two phases: a solid phase and a continuous phase. The solid phase is a buoyant, non-conducting, class A dielectric particles (homogeneous, linear, and isotropic) of solid spheres containing no free charge. The spherical particles of a diameter σ have a dielectric constant ε_p. A continuous phase is a non-conducting class A dielectric fluid of a Newtonian viscosity η_c and dielectric constant ε_c. In a suspension chosen here, polarization forces are considered to be dominant over the other forces such as colloidal forces (repulsive electrostatic and attractive van der Waals forces) and thermal forces (Brownian motions) [Adriani and Gast (1988), Brady and Bossis (1988), Klingenberg and Zukoski (1990)]. The medium fluid can influence the motion of the particles by the hydrodynamic drag. As a result, the effective forces between the particles are hydrodynamic and electrostatic forces.

In the limit of "point-dipole" approximation [Ahn and Klingenberg (1994), Klingenberg *et al.* (1989, 1991a, 1991b), Klingenberg (1993)], the electrostatic force between particle i and j is given by

$$\mathbf{F}_{ij}^{el} = F_0\left(\frac{\sigma}{R_{ij}}\right)^4 [(3\cos^2\theta_{ij}-1)\,\mathbf{e}_r + (\sin 2\theta_{ij})\mathbf{e}_\theta] \tag{1}$$

where $F_0 = 3/16\pi\varepsilon_0\varepsilon_c\sigma^2\beta^2E^2$, $\beta = (\varepsilon_p/\varepsilon_c-1)/(\varepsilon_p/\varepsilon_c+2)$, $\varepsilon_0 = 8.8542\ 10^{-12}$F/m. $\mathbf{F}_{ij}^{el}(R_{ij}, \theta_{ij})$is the electrostatic force acting on sphere i at the origin of a spherical coordinate system with a sphere j at a location (R_{ij}, θ_{ij}). Equation (1) is a governing equation explaining the particles electro- static interaction.

The influence of the electrode wall to the particles is also considered as the electrostatic interaction between a point-dipole at the sphere center and the point-dipole images of all the spheres in the suspension reflected about the wall surface.

The short-range repulsive force is introduced here to prevent the particles from overlapping. As true hard-sphere repulsion introduces extraordinary difficulty in computational load, the repulsive force on the particle i due to particle j at R_{ij} was defined as an exponential function as follows.

$$\mathbf{F}_{ij}^{rep} = F_0\exp\left[\frac{-(R_{ij}-R_m)}{0.01R_m}\right](-\mathbf{e}_r) \tag{2}$$

The repulsion between a particle and an electrode wall was treated likewise. The repulsive force on particle *i* due to the electrode surface is given by

$$\mathbf{F}_{i,wall}^{rep} = \frac{3}{16}\pi\varepsilon_c\varepsilon_p\sigma_i^2\beta^2E\exp\left[\frac{-(h_i-\sigma_i/2)}{0.01\sigma_i}\right](\mathbf{n}) \tag{3}$$

where h_i is the distance from the sphere center to the electrode surface, $\mathbf{n}$ is the unit normal vector pointing inward the fluid between electrodes.

Hydrodynamic force applied to a particle in a medium fluid is given as Stokes' drag force as follows.

$$\mathbf{F}_i^{hyd} = -3\pi\eta_c\sigma_i\left[\frac{d\mathbf{R}_i}{dt}-\mathbf{v}(\mathbf{R}_i)\right] \tag{4}$$

where $\mathbf{v}(\mathbf{R}_i)$ is the velocity field applied to a suspension. Fig. 1 shows a schematic diagram of the squeezing flow field under an electric field in the cylindrical coordinate. The squeezing flow is applied by moving the upper electrode disk to the bottom electrode with a constant speed, V_0. ER fluid is confined between two disks of radius R. As the electrode spacing H(t) between the disks decreases, the electric field E increases inversely proportional to H(t), because the applied voltage V is constant. The velocity field which was derived with the pseudosteady-state assumption in the limit of creeping flow (Re→0) is shown as follows [Denn (1980)]:

$$\mathbf{v} = v_r\mathbf{e}_r + v_z\mathbf{e}_z. \tag{5a}$$

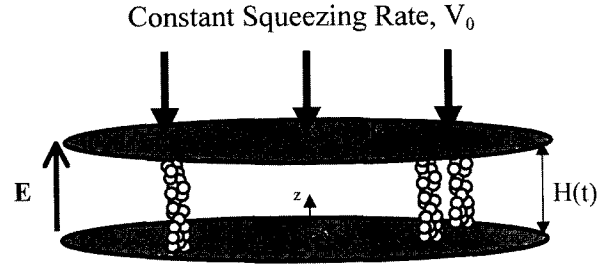

Fig. 1. Schematic view of the squeezing flow of ER fluid in cylindrical coordinate.

and,

$$\mathbf{v}_r = \frac{3rzV_0}{H^2(t)}\left(1-\frac{z}{H(t)}\right)(\mathbf{e}_r), \tag{5b}$$

$$\mathbf{v}_z = 3V_0\left(\frac{z}{H(t)}\right)^2\left(1-\frac{2}{3}\frac{z}{H(t)}\right)(-\mathbf{e}_z), \tag{5c}$$

where $\mathbf{e}_r$ and $\mathbf{e}_z$ is a unit vector in the directions of r and z in the cylindrical coordinate system, respectively. The above Newtonian flow field may not be correct for the dynamic simulation of a suspension. The existence of the particles and the formation of chain structure would affect the flow field, and this needs to be taken into account. However, there is no feasible way to incorporate this concept in the dynamic simulation as yet. Accordingly Eq. (5) was used as a first approximation in this study. In addition, the electrostatic and the repulsive forces would dominate over the hydrodynamic force in the squeezing environment, and it is expected that the perturbation of flow field would be minor in the simulation.

The motion of particle i (mass m_i) in the suspension is governed by the Newton's equation of motion as follows,

$$m_i\frac{d^2\mathbf{R}_i}{dt^2} = \sum_{j\neq i}\mathbf{F}_{ij}^{el}(R_{ij},\theta_{ij}) + \sum_{j}\mathbf{F}_{ij}^{el}(R'_{ij},\theta'_{ij}) + \sum_{j\neq i}''\mathbf{F}_{ij}^{rep}(R_{ij},\theta_{ij}) + \sum_{i}\mathbf{F}_{i}^{hyd} \tag{6}$$

where the primes in the second summation show the interaction between sphere i and the image of sphere j ; those interactions are summed over all images of all spheres, including those of sphere i. The double prime in the third summation indicates that the repulsive forces are considered between sphere i and all spheres $j \neq i$, as well as between sphere i and the electrodes. And the stress tensor is defined by

$$\langle\tau\rangle = \frac{1}{V_c}\sum_{i=1}^{N}\mathbf{R}_i\mathbf{F}_i, \tag{7}$$

where V_c is the control volume of a model suspension [Russel (1989)].

3. Numerical simulation

3.1. Simulation method

The 3-dimensional simulation of ER fluid in a squeezing flow field has been performed as follows: N particles of a diameter σ_i are placed between the electrodes of a radius R as shown in Fig. 1. The initial gap distance between the electrodes is fixed as H_0. A constant voltage is applied between two electrodes in the absence of squeezing flow, and the configuration is allowed to reach a steady state. Squeezing flow is then applied to the suspension and the normal stress can be calculated under the squeezing flow and the electric field.

The motion of the particles is governed by equation (6) which is integrated numerically with Euler's method using the dimensionless time step Δt^* ($= \Delta t/t_s$). The time step was determined based on the requirement that the simulation results are independent of the dimensionless time step. The time step has a value ranging from 0.0001 to 0.001 in our study. Also, we set the dimensionless length δ_{wall}^* in order to impose the no slip condition on the surface of the electrode disk such that a particle within δ_{wall}^* is stuck to the wall and is not allowed to move on the electrode surface. The forces between the particles were considered pairwisely only within a cutoff radius $r_c^* = 5.0$.

The upper electrode is moving downward at a constant velocity. At each time step, the dimensionless moving distance of the upper electrode, Δz^* should be decided to make the squeezing rate constant as the electric field E(t) changes with a degree of squeezing while the dimensionless time step Δz^* is held unchanged. The instantaneous squeezing rate can be written by

$$\frac{\Delta z}{\Delta t} = \frac{\varepsilon_0\varepsilon_c\beta^2E(t)^2}{16\eta_c}\frac{\Delta z^*(t)}{\Delta t^*} \tag{8}$$

and the dimensionless squeezing distance, Δz^*, should be decreased with a time evolution in order to maintain a constant squeezing rate because the electric field increases as time goes on. The material properties listed in Table 1 were used as input data for our simulation.

3.2. Effect of parallel processing

In this research, Message Passing Interface (MPI) was used to overcome the limitation of considering the small number of particles in a dynamic simulation [Cornell Theory Center(1995), Hwang and Degroot(1989), Walker (1995)]. Before going further, the effect of parallel processing will be investigated in advance.

The effect of parallel processing with MPI was investigated by comparing the calculating time with respect to the number of nodes. First, the number of particles N

Table 1. List of properties used in the simulation

GEOMETRICAL PROPERTIES AND ELECTRICAL CONDITIONS	
Electrode diameter	D = 50 mm
Initial gap distance	H_0 = 1.0 mm
Squeezing rate	V_0 = 1.0 mm/sec
Applied voltage	V = 1.0 kV
PARTICLE PROPERTIES	
Diameter	σ = 100 μm
Dielectric constant	ε_p = 23.4
CONTINUOUS PHASE PROPERTIES	
Viscosity	η_c = 0.01 Pa·sec
Dielectric constant	ε_c = 7.3

(= 1440, 2480, 3200, 4800) was increased at each number of node (1 to 16). The volume fraction was in the range between 0.03 and 0.13. Secondly, the effect of the number of nodes used in MPI calculation was investigated in the same way. The number of nodes (= 1, 2, 4, 8,16) was increased at each identical number of particles. In each case, the calculating time was measured at 1000 dimensionless time steps. As shown in Fig. 2 and Fig. 3, the doubling of the number of particles required about 4 times of the calculating time in this range, while the doubling of the number of nodes shows about 2 times of the calculating speed. This effect could be clearly observed in the case of relatively large number of particles used. Consequently, the more particles were used in the simulation, the more nodes were needed to reduce the real calculating time. The simulations in the next section were carried out with 10 nodes.

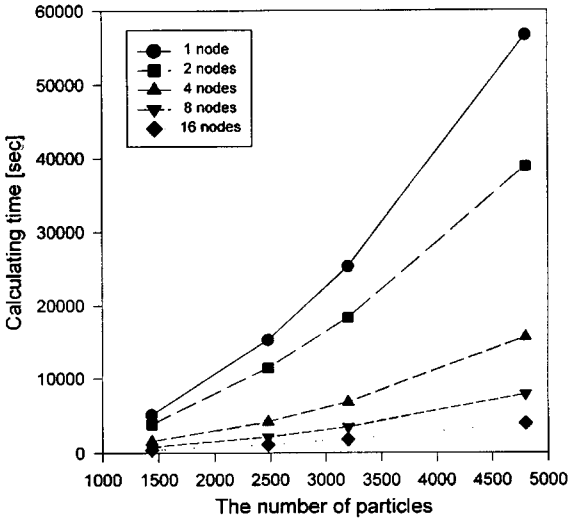

Fig. 2. Effect of the number of monodisperse particles in the case of various nodes in MPI calculation (1000 time steps).

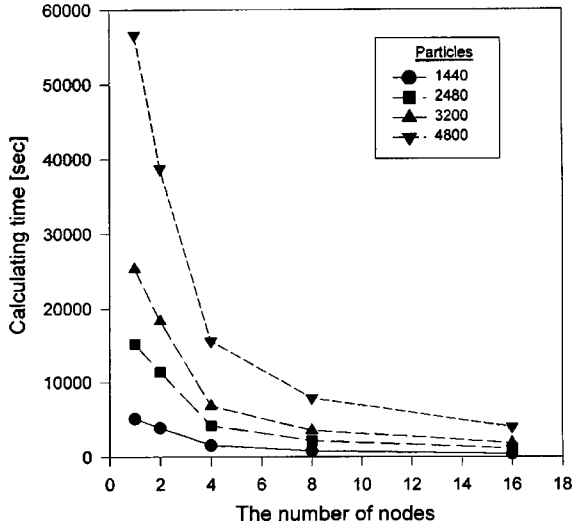

Fig. 3. Effect of the number of nodes used in MPI calculation in the case of various monodisperse particles (1000 time steps).

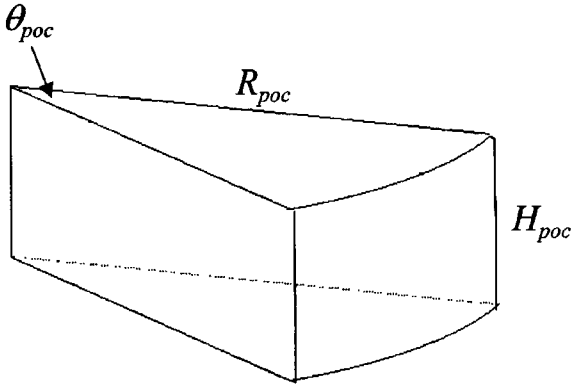

Fig. 4. Schematic view of a Piece-of-Cake space.

4. Results and discussion

4.1. Evaluation of the POC approximation

The POC-shaped space is a part of the whole domain between the electrodes, and relatively smaller number of particles is needed for this simulation. Its schematic view is shown in Fig. 4. This approximation significantly reduces the computational load. As no boundary condition was imposed on the boundary of the "POC" space, it is necessary to investigate the boundary effect in the θ- and R-direction, even though it predicts some important characteristics of ER fluids. The angle was varied from $\pi/16$ to $3\pi/16$. First, five different random initial configurations were considered to investigate the effect of the initial configuration. The center angles were set identical ($\theta_{poc} = \pi/16$) and the other conditions being the same (radius $R_{poc} = 5.0$ mm, height $H_{poc} = 1.0$ mm, and applied voltage $V = 1.0$ kV). Squeezing rate of $V_0 = 1.0$ mm/sec was applied after the particles formed the chain-like structure in the equilibrium state. The result is plotted in Fig. 5. The effect of random initial configuration seems to be negligible, as there exists no significant difference between the five curves in terms of the magnitude of stress per the number of particles as well as the behavior of the stress oscillation. Some stress components are given together for comparison. The rr-component of the stress is nontrivial only at high strain region, and the corresponding normal stress difference looks similar with the zz-component of the stress tensor. Secondly, five different POC-shaped spaces were introduced to investigate the θ-directional effect: One random initial configuration was chosen and θ_{poc} were changed as $\pi/16$, $2\pi/16$, $3\pi/16$, $4\pi/16$, and $8\pi/16$, respectively. The number of particles N (= 233, 466, 699, 932, 1864) was increased with the angle to make the solid volume fraction constant, while the other conditions remaining the same: $R_{poc} = 5.0$ mm, $H_{poc} = 1.0$ mm, $V = 1.0$ kV, and $V_0 = 1.0$ mm/sec. The stresses shown in Fig. 6 show nearly the same

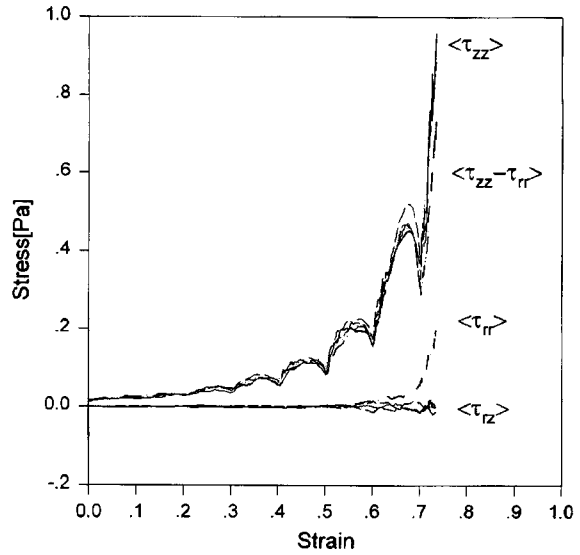

Fig. 5. Normal and shear stresses of a suspension with 233 monodisperse particles; various lines mean different initial configurations. Squeezing rate is 1.0 mm/sec.

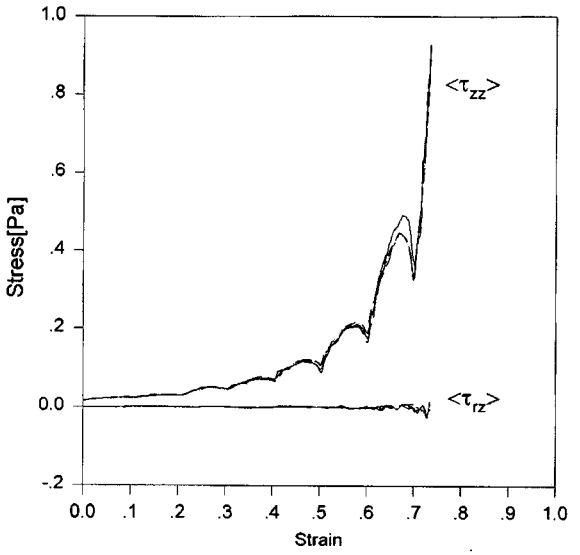

Fig. 6. Normal and shear stresses of a suspension with 233(–)/466(- -)/699(---)/932(-·-)/1864(···) monodisperse particles. Squeezing rate is 1.0 mm/sec.

behavior in terms of the magnitude of the stresses per the number of particles as well as the position of each stress peak. The boundary effect in θ-direction seems to be negligible based on this observation, and the results obtained in a "POC-shaped" space well represent the characteristics in the whole electrode space in terms of the behavior of the normal and shear stresses.

4.2. Suspension model in the whole domain

In order to investigate the macroscopic behavior of ER

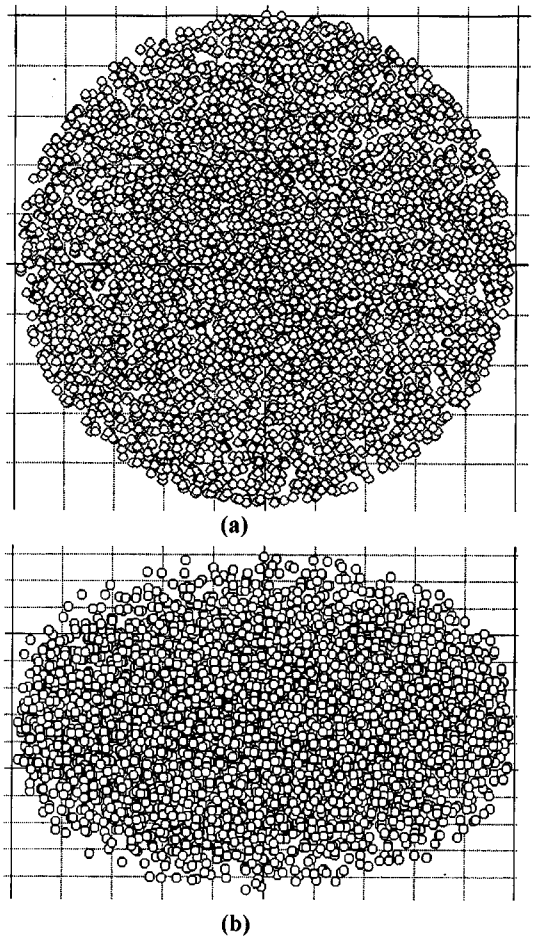

Fig. 7. Snapshot of a random initial suspension with 3740 monodisperse particles in the top view (a) and perspective view (b).

fluid under squeezing flow, 3740 particles were randomly distributed in the electrode disk whose geometric constants are $\theta_{poc} = 2\pi$, $R_{poc} = 2.5$ mm, and $H_{poc} = 1.0$ mm (Fig.7). Particle volume fraction is 0.1. In the same way, a constant voltage V = 1.0 kV was applied to the suspension before squeezing proceeds.

Upon application of the electric field, random configuration evolves into an initial configuration (Fig.8). Various types of structures were observed in the equilibrium state. They include single chains as well as multiple chains that are composed of several single chains. During the equili bration process, the normal stress increases a little (Fig.9). Once squeezing starts to be applied to this configuration at the rate of 1.0 mm/sec, the chains are deformed both radially and axially in the same way as discussed in a regular configuration [Kim *et al.* (1999)]. The chains near the center of disk are compressed near the original position without flowing in a radial direction, and the chains located far from the center show relatively large amount of movement in a radial direction as shown in Fig.10. The chains may merge into one large chain, or one chain may be divided

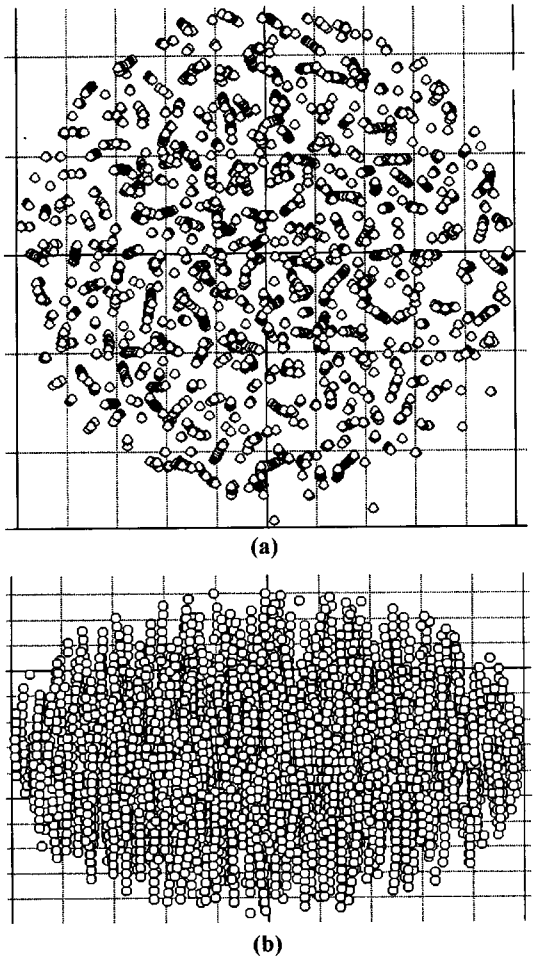

Fig. 8. Snapshot of a random equilibrium suspension with 3740 monodisperse particles in the top view (a) and perspective view (b) after the electric field is applied.

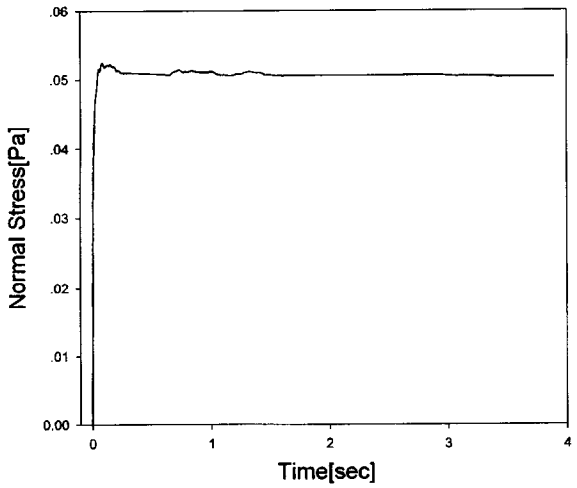

Fig. 9. Normal stress of a suspension with 3740 monodisperse particles. Applied Voltage is 1.0 kV.

into two or more chains that are immediately added to the next chains. This chain-to-chain interaction can also be

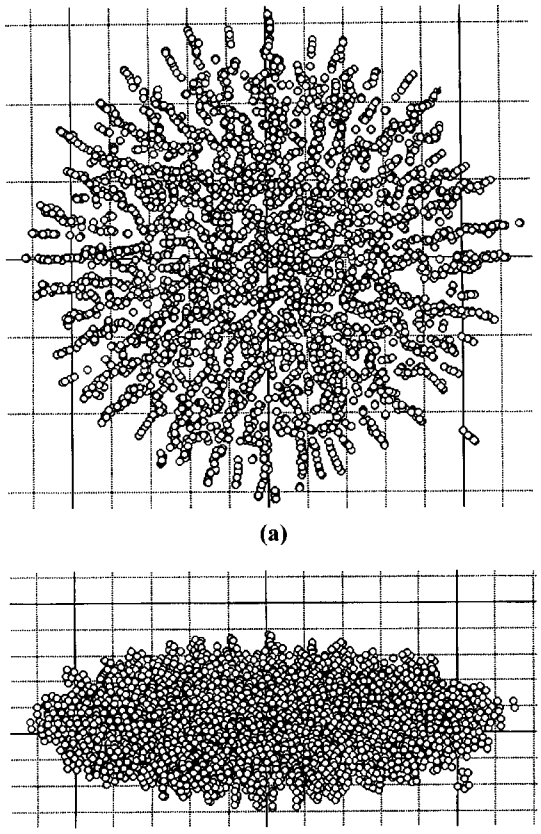

Fig. 10. Snapshot of a final suspension with 3740 monodisperse particles in the top view (a) and perspective view (b) at strain=0.65. Squeezing rate is 1.0 mm/sec.

observed experimentally. The radial flow tends to move the particles in its direction while the particles are activated electrically, and it promotes aggregation due to the electrostatic attractions. The macroscopic rearrangement is more dramatic in the region far from the center where the radial flow field is stronger. As the electrode gap becomes narrower, each rib-like configuration becomes thicker and stronger due to the increase of the electric field. At a certain strain, it is possible that a very stable macroscopic structure is formed between the electrodes. In other words, the chains in a suspension reach a configuration that can bear the squeezing pressure.

As seen in Fig.11, a yield behavior is observed without an overshoot at the beginning of the squeezing, and the oscillation of the normal stress is hardly observed in an earlier stage. It seems that each chain-like structure develops a different mode of stress and thus the different stress curves are reduced into a smooth curve by overlapping. Therefore, increasing randomness may decrease the oscillation of the stresses.

4.3. Comparison with the experimental result

Chu *et al.* (2000) carried out an experimental study on

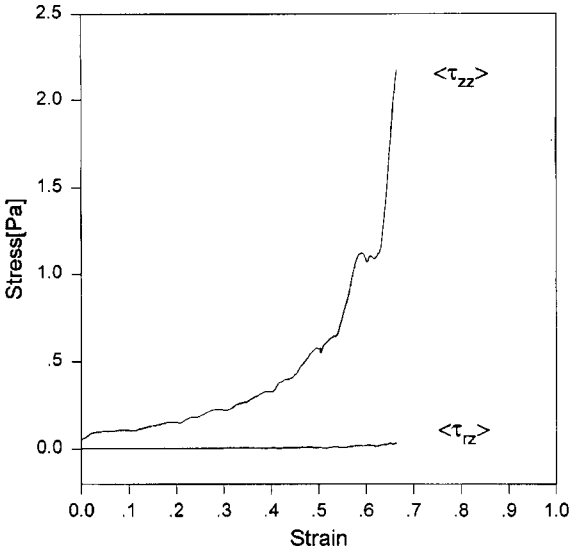

Fig. 11. Normal and shear stresses of a suspension with 3740 monodisperse particles. Squeezing rate is 1.0 mm/sec.

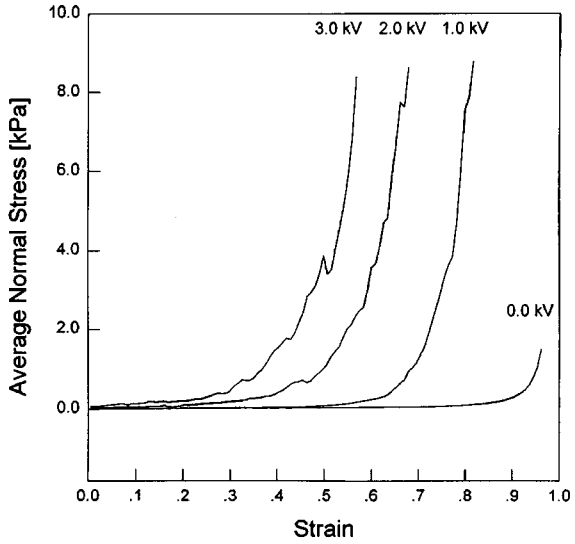

Fig. 12. Average normal stresses versus strain for DV10 at various voltage inputs.

the squeezing flow of ER fluids. According to this study, the high yield behavior could be obtained by applying a squeezing flow on the ER suspension composed of silica in silicon oil. The increase of electric field and volume fraction during the squeezing process increases the strength of structures formed between the electrode gap, leading to the increase of normal stresses. Also, large normal stresses could be obtained in the case of high voltage, high volume fraction, low medium viscosity, and high water content.

In the experiment, the initial gap between two parallel plates is 2.0 mm. Fig.12 can be compared with the prediction of a dynamic simulation. Each case of a random configuration and a regular configuration with 10 volume percent shows different response of normal stresses. No overshoot of the stress was observed in the random configuration (Fig.11), while it was observed in the regular configuration (Fig. 13). Also, the oscillation of stress, which can be observed in the regular configuration, diminishes slowly by the overlapping of the different modes of stresses in the random configuration. It is qualitatively in good agreement with the experimental result. However, the magnitude of the stress in the random configuration is smaller than that in the regular case. The increase of randomness in structure decreases the oscillation of stress, while the decrease of randomness increases the magnitude of the stress.

5. Conclusion

Message Passing Interface (MPI), which is one of the most widely-used parallel processing techniques, has been employed in a dynamic simulation of ER fluid under squeezing flow. As the number of particles used in

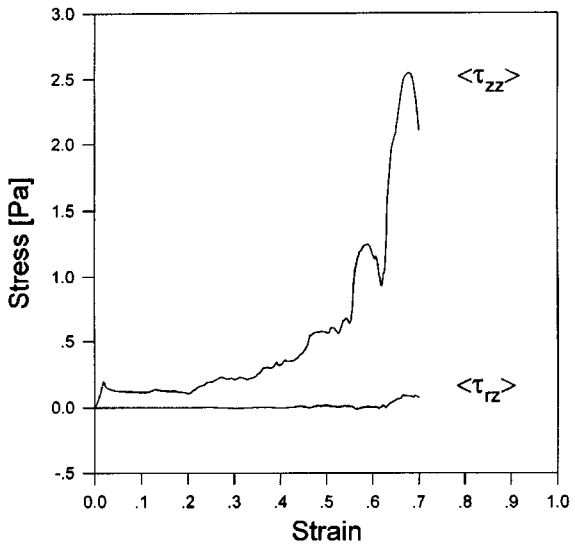

Fig. 13. Normal and shear stresses of a regular suspension arranged in the r-direction (N=960). Squeezing rate is 1.0 mm/sec.

the simulation could be increased significantly, full domain between the electrodes has been covered. The numerical treatment or the approximation used to reduce the computational load has been evaluated for its validity. The POC approximation that accounts only for the part of the whole domain between the electrodes and simulates the ER behavior reasonably well at a much reduced computational load has been evaluated for its validity and was found to be quite effective. As the number of particles is increased, the fluctuation of the normal stress becomes diminished and the prediction in general was found to be in good agreement with the experimental results.

6. Nomenclature

Alphabetic symbols

E : applied electric field, kV/mm
$\mathbf{e}_\theta$: unit vector in the direction of θ
$\mathbf{e}_r$: unit vector in the direction of r
$\mathbf{e}_z$: unit vector in the direction of z
$\mathbf{F}_{ij}^{el}$: electrostatic force between sphere i and sphere j and the electrode surface, N
$\mathbf{F}_{ij}^{rep}$: repulsive force on particle i due to particle j and the electrode surface, N
$\mathbf{F}_i^{hyd}$: hydrodynamic force applied to particle i in a medium fluid, N
F_0 : $3/16\pi\varepsilon_c\varepsilon_p\beta^2E^2$ in equation (1), N
H : gap separation, m
H_0 : initial gap separation, m
H_{poc} : height of POC-shaped space, mm
m_i : mass of particle i, kg
N : number of particles
r_c^* : cutoff radius
R : electrode radius, m
R_{ij} : distance between particle i and j in spherical coordinates, m
R_m : mean diameter, m
R_{poc} : radius of POC-shaped space, mm
t_s : characteristic time, sec
Δt^* : dimensionless time step
v_r : velocity field applied to a suspension in the direction of r, m/sec
v_z : velocity field applied to a suspension in the direction of z, m/sec
V : applied voltage, kV
V_0 : squeezing rate, m/sec
Δz^* : dimensionless squeezing distance

Greek symbols

α : ratio of the dielectric constant of the particles to that of the continuous phase
β : dielectric mismatch
γ : strain
δ_{wall}^* : dimensionless length of no slip boundary condition
ε_c : dielectric constant of the base fluid
ε_{poc} : dielectric constant of the particle
ε_0 : permittivity of vacuum ($=8.8542\times10^{-12}$), F/m
θ_{ij} : angle between particle i and j in spherical coordinates, radian
θ_{poc} : angle of POC-shaped space, radian
η_c : viscosity of the base fluid, Pa·sec
σ_i : diameter of particle i, m
$\langle\tau_{rz}\rangle$: shear stress of the component rz, Pa
$\langle\tau_{zz}\rangle$: averaged normal stress against the squeezing force, Pa

7. References

Adriani, P.M. and A.P. Gast, 1988, "A microscopic model of electrorheology," *Phys. Fluids* **31**, 2757.

Ahn, K.H. and D.J. Klingenberg, 1994, "Relaxation of polydisperse electrorheological suspensions," *J. Rheology* **38**, 713.

Brady, J.F. and G. Bossis, 1988, "Stokesian dynamics," *Ann. Rev. Fluid. Mech.* **20**, 111.

Brooks, D.A., 1994, "Selection of Commercial Electro-rheological Device," in *Proceedings of the Fourth International Conference on Electrorheological Fluids*, ed. by R. Tao and G.D. Roy, World Scientific, Singapore, 643.

Chu, Sang-Hyon, Kyung Hyun Ahn, and Seung Jong Lee, 2000, "An experimental study on the squeezing flow of electrorheological suspensions," *J. Rheology* **44** (in press).

Cornell Theory Center, 1995, http://www.tc.cornell.edu/Smart-Nodes/Newsletters/MRI.series/.

Denn, M.M., 1980, Process Fluid Mechanics, Prentice-Hall, New Jersey.

Havelka, K.O. and J.W. Pialet, 1996, Electrorheological technology: The future is now, *CHEMTECH* June, **36**, 36.

Hwang, K. and D. Degroot, 1989, Parallel processing for supercomputers and artificial intelligence, McGraw-Hill.

Kim, Do Hoon, Sang-Hyon Chu, Kyung Hyun Ahn, and Seung Jong Lee, 1999, "A dynamic simulation on the squeezing flow of ER fluids," *Korean Journal of Rheology* **11**, 82.

Klingenberg, D.J. and C.F. Zukoski IV, 1990, "Studies on the Steady-Shear Behavior of Electrorheological Suspensions," *Langmuir* **6**, 15.

Klingenberg, D.J., 1993, "Simulation of the dynamic oscillatory response of electro-rheological suspensions: Demonstration of relaxation mechanism," *J. Rheology* **37**, 199.

Klingenberg, D.J., F. van Swol, and C.F. Zukoski, 1989, "Dynamic simulation of electro-rheological suspensions," *J. Chem. Phys.* **91**, 7888.

Klingenberg, D.J., F. van Swol, and C.F. Zukoski, 1991a, "The small shear rate response of electrorheological suspensions. I. Simulation in the point-dipole limit," *J. Chem. Phys.* **94**, 6160.

Klingenberg, D.J., F. van Swol, and C.F. Zukoski, 1991b, "The small shear rate response of electrorheological suspensions. II. Extension beyond the point-dipole limit," *J. Chem. Phys.* **94** 6170.

Lukkarinen, A. and K. Kaski, 1998, "Simulation studies of electrorheological fluids under shear, compression, and elongation loading," *J. Appl. Phys.* **83**, 1717.

Russel, W.B., D.A. Saville, and W.R. Schowalter, 1989, Colloidal Dispersions, Cambridge.

Sproston, J.L., R. Stanway, and A. Faghmous, 1991, "The electrorheological effect and its industrial application," *Rev. Gen. Electr.* Sept., 21.

Walker, D.W., 1995, http://www.epm.ornl.gov/~walker/mpi/.